Reducing the Effect of Load Torque Disturbances in Dual Inertia Systems with Lost Motion

Peter Schmidt
Rockwell Automation
1201 S. 2nd St.
Milwaukee, WI 53204

Thomas Rehm
Rockwell Automation
6400 W. Enterprise Dr.
Mequon, WI 53092

***Abstract* — Industrial motor drives and controllers are connected to a variety of applications. Dual inertia systems with lost motion are particularly hard to model and control. This paper discusses the utilization of acceleration feedback to reduce the effects of load torque disturbances and stabilize the plant output. Following theoretical analysis and simulations, two experimental test stands were utilized to demonstrate the effectiveness of the solution.**

I. INTRODUCTION

Industrial motor drive applications that connect a motor to a load utilizing gears, ball screws, and/or belts experience many different forms of disturbance in the system. Dual inertia resonant systems have been modeled [1-7], and a variety of control schemes presented [2] to eliminate or reduce this effect.

Limit cycle instabilities that are generated in plants with backlash have also been modeled as hysteretic systems. However, some of the more difficult disturbances to control are the ones that can be modeled as both dual inertia resonant systems with lost motion [8-12]. The lost motion can be thought of as dead-zone, backlash, or some other type of non-linear behavior where changing direction of the motion momentarily decouples the motor from the load. Observations have been made in the system when reducing the acceleration or deceleration command can also decouple the motor from the load.

The control objective is to design a system such that 1) the ideal admittance to a command input is unity $Y_{ref}(s) = 1$ and 2) the ideal admittance to a load disturbance is zero $Y_{load}(s) = 0$. Every effect observed on the output of the system is equal to the cause times the admittance. This also relates nicely to Newton's third law: every action has an equal (in magnitude) and opposite (in direction) reaction.

Designing a controller and the commands necessary to track a command trajectory has been demonstrated in many papers over the years. This paper will consider disturbance rejection of dual inertia systems with lost motion.

There are two choices, or a combination of them, to reduce the effects of disturbances in a system: reduce the cause or reduce the admittance. Reducing the cause implies that one has some control over the plant loads or source of the disturbance. If this were the case, then the cause could be included with the other manipulated variables. The intent of this paper is to revisit disturbance rejection and determine a way to make the system appear stiffer to unwanted loads.

The simple block diagram in Fig. 1 defines a velocity PI regulator and plant modeled as inertia Jp.

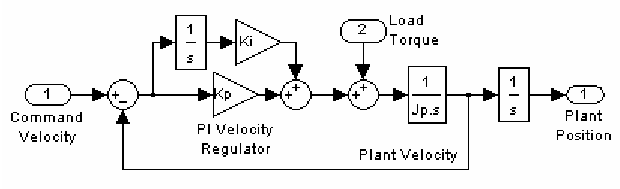

Fig. 1. PI velocity regulator & plant inertia

Stiffness is defined as the transfer function between load torque disturbance τ_L and plant position θ:

$$\frac{\tau_L(s)}{\theta(s)} = J_p s^2 + K_p s + K_i \qquad (1)$$

Increasing the integral and proportional control gains will increase the stiffness in the low and middle frequency regions respectively. Increasing the plant inertia will effectively increase the stiffness in the high frequency region as shown in Fig. 2.

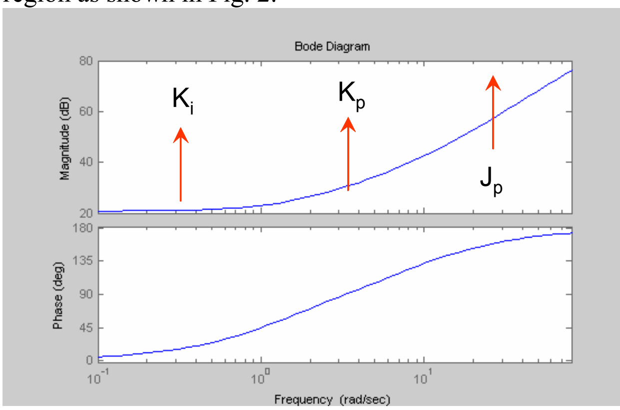

Fig. 2. Stiffness plot

The controller for the previous plot was designed to have two poles at 1 rad/sec and 10 rad/sec to demonstrate the concept of stiffness. The graph clearly shows the breaking points in the magnitude and phase plots at 1 and 10 rad/sec. Stiffness has been described in [13].

A. Plant Model Definition

This paper addresses the principals of admittance as it affects position and/or velocity ripple caused by torque disturbances in dual inertia systems with lost motion. Fig. 3 is a block diagram of a dual inertia system with lost motion.

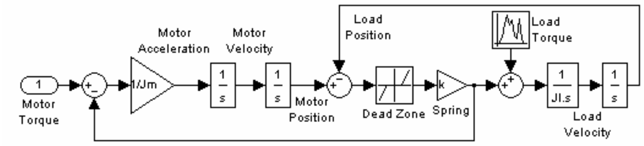

Fig. 3. Motor-load model with lost motion

The lost motion was modeled as dead zone using the Simulink block of the same name. A similar model can be seen in [8]. This function coupled with the resonant spring modeled the real world behavior fairly accurately. By commanding a simple trapezoidal velocity profile and plotting the difference between the command position and motor position as well as the difference between the motor and load positions, the resonance/lost motion that exists in the plant can be observed in Fig. 4.

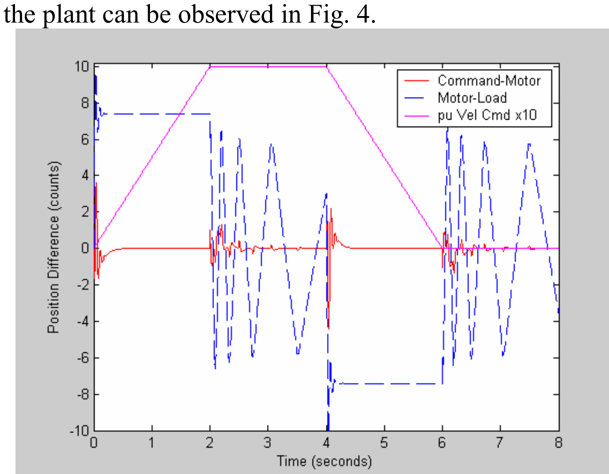

Fig. 4. Resonance/lost motion in a trapezoidal velocity profile

The deadzone was set to 0.5 degrees. With an encoder feedback set to 4096 counts per revolution, that corresponds to approximately six counts of lost motion. The graph demonstrates the resonant/lost motion between the motor and load. As soon as torque is removed from the motor inertia, the load inertia stops accelerating and the spring in the system causes the inertias to start resonating. The per unit (pu) velocity command signal is also plotted to indicate how the position differences are affected by the command signals.

The inertia values are chosen and set using per unit notation. In the per unit system: inertia has units of seconds, rated torque equals one (unit-less) and rated speed equals one (unit-less).

B. Acceleration Feedback

The benefits of utilizing acceleration feedback in a motor drive have been demonstrated in [13-15]. When acceleration feedback is implemented in the controller, the effective plant inertia can be electrically increased in place of mechanically adding inertia to the plant. System stability is then improved and the speed bandwidth may be increased with increased stiffness.

An acceleration signal is typically not available in a motor drive. This signal could be generated by differentiating a known signal such as position or velocity. Differentiation creates noise in a signal and typically requires additional filtering which introduce phase lag in the system.

Acceleration could also be estimated by utilizing a state observer [13]. However, with the introduction of lower cost high resolution feedback devices, differentiation of position to obtain velocity and acceleration signals has become acceptable.

A system model of the mechanical plant from Fig. 3 was connected to a controller that was designed to have cascaded position, velocity, and current regulators. This block diagram is shown in Fig. 5.

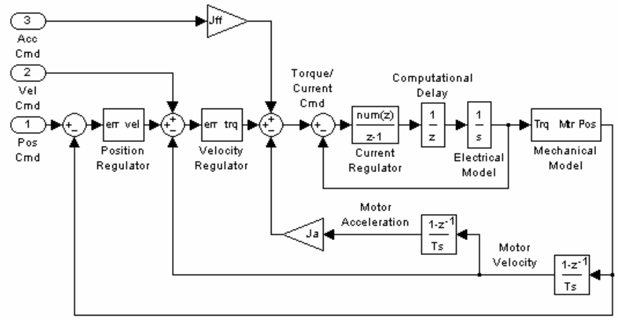

Fig. 5. Cascaded position, velocity, & current regulators with state observer

From the block diagram, one can observer the addition of the acceleration loop to the controller. The velocity and acceleration signals were found by differentiation.

Section II develops the theory and simulations when acceleration feedback is applied to the dual inertia system with lost motion. Section III provides results on two physical test beds that were developed. Finally in Section IV, conclusions are drawn based on the observations from this work.

II. THEORY & SIMULATIONS

The block diagram from Fig. 5 was simulated to produce motor/load output positions and velocities. The simulation parameters are shown in Table 1.

TABLE 1.
SIMULATION PARAMETERS

Parameter	Value	Units
Vel. loop sample period	0.5	msec
Cur. loop sample period	0.25	msec
Computational delay	0.18	msec
Base speed	1000	RPM
Encoder feedback	4096	CPR
Motor inertia	0.117	sec
Load inertia	0.863	sec
Resonant frequency	65	Hz
Anti-res. frequency	22.5	Hz
Backlash	0.5	Degrees
Pos. loop bandwidth	3	Hz
Vel. loop bandwidth	15	Hz
Cur. loop bandwidth	318	Hz

A state observer was not implemented because, as a simulation, there is no noise generated when the feedback signal is differentiated. Instead, the simulation insured that the quantization error created by the finite number of feedback pulses from the encoder (4096) was incorporated into the velocity and acceleration signals when they were differentiated.

The pu results for following a trapezoidal velocity are shown in Fig. 6.

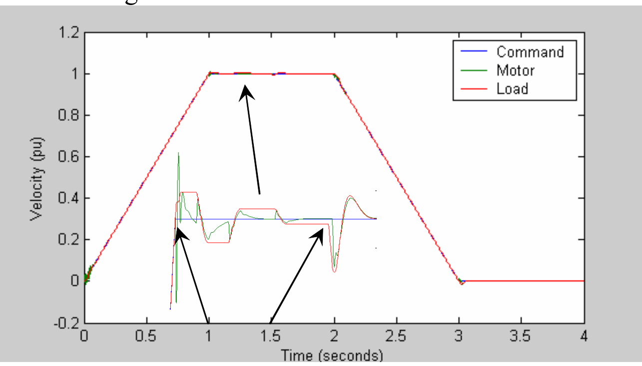

Fig. 6. Trapezoidal velocity profile with a step load

At 1 second the velocity stops ramping and there is a slight overshoot by the load. At 1.5 seconds a 50% step in load torque disturbance was applied to the load inertia. The graph shows a slight oscillation caused by the disturbance.

The corresponding applied motor torque signal (current) and the inertia stabilization signal (acceleration feedback) are shown in response to the velocity command and load torque disturbance in Fig. 7 all as pu signals.

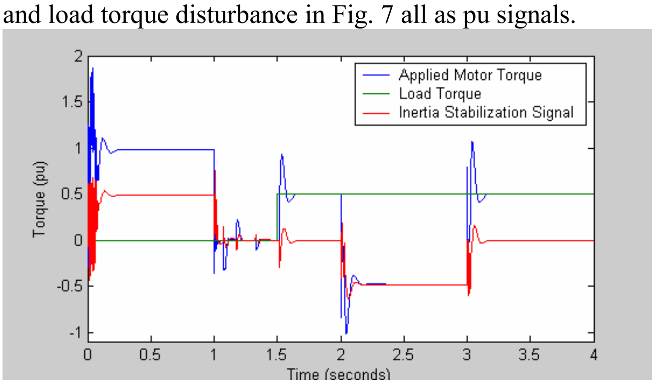

Fig. 7. Motor torque/current signals, load, & acceleration compensation signal

The load torque disturbance is shown as a step occurring at 1.5 seconds. The inertia stabilization signal is non-zero when it is trying to compensate the motor feedback signal during accelerating/decelerating periods.

If the acceleration signal was not fed back to the controller, the system would become unstable. If the velocity loop bandwidth was reduced to 1-2 rad/sec, the system could be stabilized, but would remain highly oscillatory.

Previous works [2] and [13] have shown that acceleration feedback improves system stiffness in the high frequency region, typically above the velocity loop bandwidth. The amount of stiffness that can be added to the system is a function of the quality of the acceleration signal, filters, and sampling period.

III. EXPERIMENTAL RESULTS

Two experimental test beds were utilized to verify that acceleration improved the disturbance response of the system. The first test stand was a dynamometer that did not have any measurable lost motion in it. The test and load motors were tightly coupled. The second test stand did have lost motion. The second experimental platform was designed to model a printing press operation where high frequency disturbances are a major problem with print registration.

A. Dynamometer Test Stand

A dynamometer test stand was utilized to verify the increase in performance due to the addition of acceleration feedback. The autodyne is shown in Fig. 8.

Fig. 8. AutoDyne test stand

An AC test motor was connected to a Himmelstein torque transducer through a flexible coupling. The Himmelstein was also connected through a similar coupling to a DC load motor. The Himmelstein was able to provide the actual torque applied from the test motor to the load motor. In addition, the speed of the dyne could also be monitored. Table 2 contains the dyne motor information.

TABLE 2.
AUTODYNE MOTOR DATA

AC Test Motor	Units	DC Load Motor
1329RS-2A00318VNC-DH	Catalog #	1325LS-DD01018DGH-CC-RL T1
3	HP	10
460	Volt	500
1726	RPM	1750
4.4	FLA	17.4
108	in-lb	

B. Acceleration Test

In the first test, the motor is at zero speed and is commanded to reach rated speed with a drive acceleration time programmed for 0.1 seconds. This command will overdrive the motor and the torque/current signal will become saturated. This test is utilized to determine whether the drive can maintain control of the motor.

The dyne has 1.03 seconds of total system inertia in the per unit system. This implies that it will take 1.03 seconds to reach rated speed when rated torque is applied to the motor. Rated speed is 1 pu and rated torque is 1 pu.

This test is used to determine whether the drive can accelerate 150% load and maintain regulation during the acceleration ramp. The velocity loop bandwidth was tuned for 100 rad/sec. The acceleration feedback signal was disabled for the first pass through this test. The results are shown in Fig. 9.

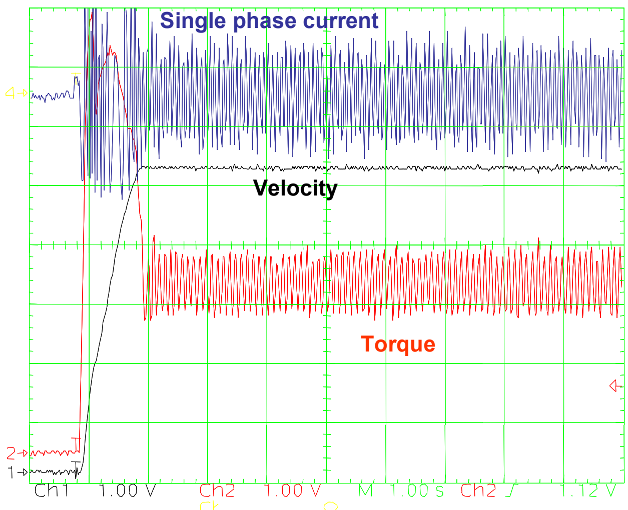

Fig. 9. Accelerate with 150% load and acceleration feedback disabled

The top trace shows a single phase current signal in the stationary reference frame from the motor. The middle trace shows the velocity ramping up from zero to rated speed (1 V = 351 RPM). The bottom trace is the measured motor torque applied to the load (1 V = 59 in-lb). Frequency oscillations of approximately 10 Hz in the mechanical system are clearly visible in the measured torque. These oscillations will have a negative effect on the system performance and show up as ripple in the velocity response.

The same test was conducted with the acceleration feedback loop enabled. The results are shown in Fig. 10. The top trace again shows a single phase current. The middle velocity trace exhibits a similar profile. What is not definitively shown is a reduction in the velocity ripple. However, the torque signal applied to the load clearly demonstrates that there is considerably less noise in the system. The oscillations are reduced in magnitude between 75-80 percent.

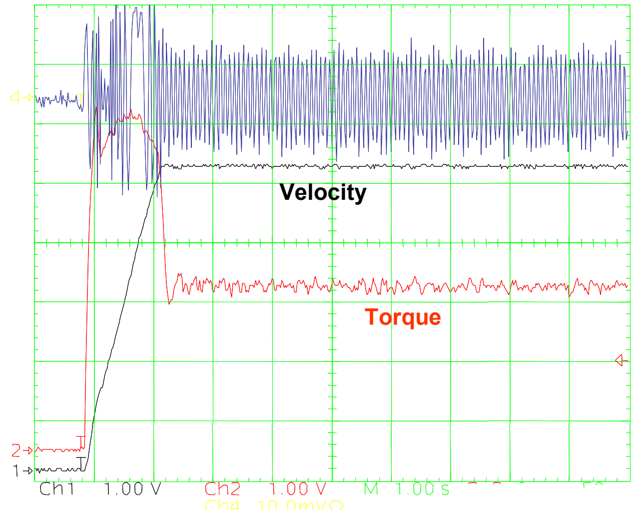

Fig. 10. Accelerate with 150% load in 0.1 seconds with acceleration feedback enabled

C. Shock Load Test

In the next test, a 150% shock load was applied by the load motor to the test motor. The test motor was running at rated speed when the load was applied. The velocity loop bandwidth was set for 100 rad/sec. The following scope traces show the results without, Fig. 11 and with, Fig. 12, acceleration feedback enabled.

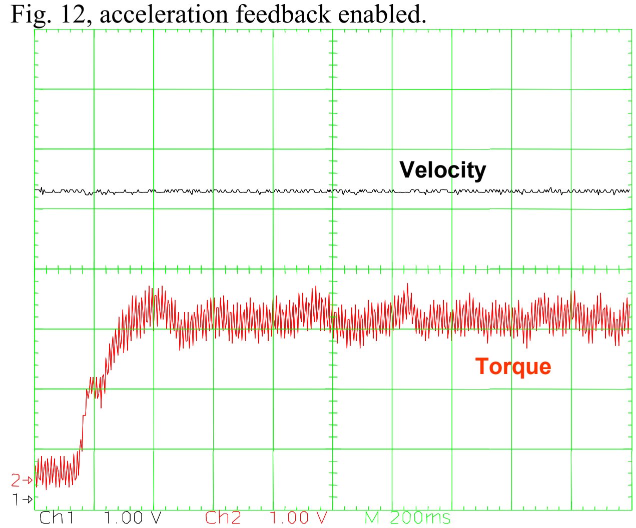

Fig. 11. 150% Shock load applied to motor with acceleration feedback disabled

The top traces are the velocity signal maintaining constant rated speed. The bottom trace in Fig. 11 demonstrates the noise that is present in the torque signal with acceleration feedback disabled. The bottom trace in Fig. 12 shows a reduction in the torque ripple with acceleration feedback enabled.

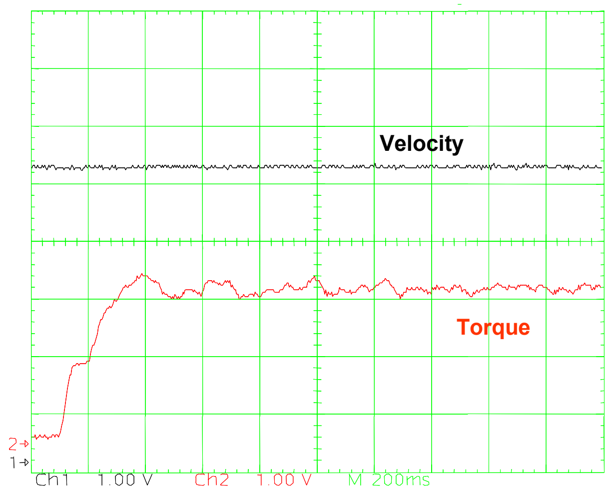

Fig. 12. 150% Shock load applied to motor with acceleration feedback enabled

Similar to the first test, acceleration feedback greatly reduces the amount of noise due to resonance and lost motion in the system as shown by these two tests.

If the velocity loop bandwidth is relaxed to 30 rad/sec, the velocity feedback can be shown to droop slightly when the shock load is applied. These results are shown in Fig. 13 by combining the two scope traces into one.

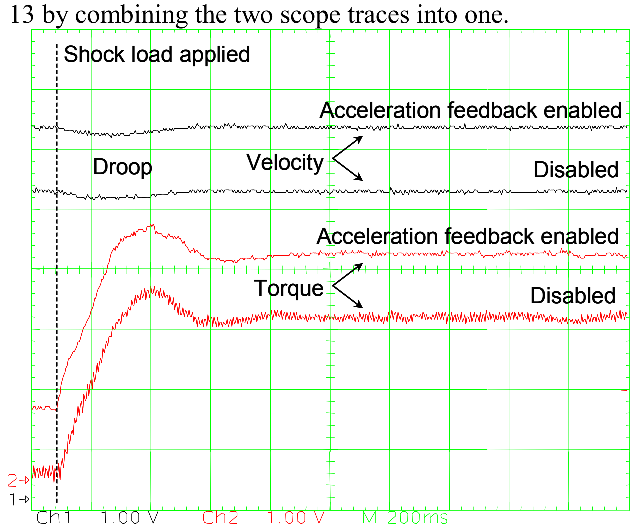

Fig. 13 150% Shock load applied to motor with acceleration feedback enabled/disabled, 30 rad/sec bandwidth

The torque signal shows more noise when the acceleration feedback signal is disabled.

D. Experimental Test Stand

The second experimental test stand was built to simulate a real printing web application. The test motor was a 5.5 kW induction motor with a base speed of 1000 RPM. The position feedback device was a Stegmann encoder with feedback of one million counts per revolution. Because of the high resolution feedback device, the velocity and acceleration signals were found by differentiating the position signal. Applying the appropriate filtering on the feedback signals becomes a critical part of the closed loop performance of the system.

The test motor was connected to a high precision planetary gearbox with a gear ratio of 3:1. The gear box was then connected to a flexible coupling that was attached to two large inertial wheels. The wheels had a reflected inertia back to the motor of 8:1. Finally, a programmable load motor was connected to the drive shaft via a belt.

There were approximately 150 counts of lost motion or 3.24 arc minutes of backlash in the gearbox. Consequently the resonant frequency varied from 0 up to approximately 90 Hz. If the gears are not engaged, then there is no coupling between the motor and load and the resonance is zero. Depending upon the amount of loading, the resonance could approach 90 Hz. This experimental test stand is shown in Fig. 14.

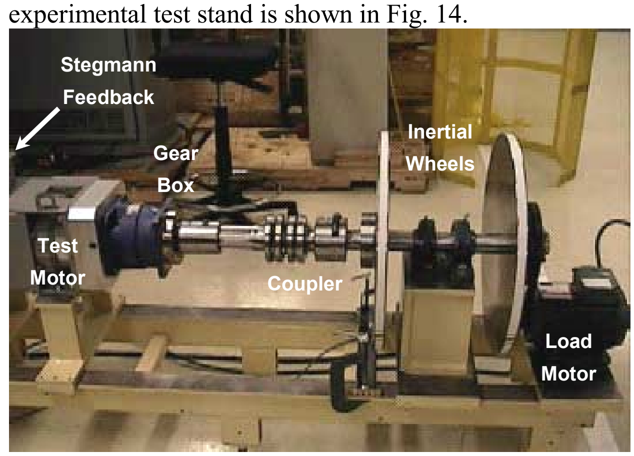

Fig. 14 Experimental test setup: dual inertia system with resonance (shaft) and lost motion (gear box & coupler)

For this experimental system, a maximum velocity loop bandwidth of 140 rad/sec was achieved with acceleration feedback enabled. Without acceleration feedback, a bandwidth of only 30 rad/sec was maintained before the system went unstable.

IV. CONCLUSIONS

Dual inertia systems with lost motion generate high frequency noise that can cause the system to go unstable and severely limit the bandwidth/performance of the system. The lost motion in the gear train compounded with the flexible coupling in the system introduces multiple frequencies that must be reduced or eliminated. Acceleration feedback has been shown to greatly reduce the disturbances present in these types of systems. In addition, the velocity loop bandwidths of the system can be increased to improve the baseband performance of the system.

V. ACKNOWLEDGMENTS

The authors gratefully acknowledge the work performed by Jeff Fell from the Rockwell Automation Test Laboratory, Mequon. His expertise in the preparation, execution, and monitoring of the tests and results was greatly appreciated.

VI. REFERENCES

[1] G. Ellis, Z. Gao, “Cures for Low-Frequency Mechanical Resonance in Industrial Servo Systems”, Proceedings of IEEE Industrial Applications Society Annual Conference, Chicago, IL, Sep./Oct. 2001, pp. 252-258

[2] G. Ellis and R. Lorenz, “Resonant Load Control Methods for Industrial Servo Drives”, Proceedings of IEEE Industrial Applications Society Annual Conference, Rome, Italy, Oct. 2000, pp. 1438-1445

[3] A. Matsubara, Y. Kakino, and Y. Watanabe, “Servo Performance Enhancement of High Speed Feed Drives by Damping Control”, Proceedings of Flexible Automation Conference, Ann Arbor, MI, Jul. 2000

[4] G. Zhang, “Comparison of Control Schemes for Two-Inertia System”, IEEE Conference on Power Electronics and Drive Systems, PEDS 99, Hong Kong, Jul. 1999, pp. 573-578

[5] Y. Hori, H. Sawada, and Y. Chun, “Slow Resonance Ration Control for Vibration Suppression and Disturbance Rejection in Torsional System”, IEEE Transactions on Industrial Electronics, Vol. 46, No. 1, Feb. 1999, pp. 162-168

[6] P. Korondi, H. Hashimoto, and V. Utkin, “Direct Torsion Control of Flexible Shaft in an Observer-Based Discrete-Time Sliding Mode”, IEEE Transactions on Industrial Electronics, Vol. 45, No. 2, Apr. 1998, pp. 291-296

[7] K. Sugiura and Y. Hori, “Vibration Suppression in 2- and 3-Mass System Based on the Feedback of Imperfect Derivative of the Estimated Torsional Torque”, IEEE Transactions on Industrial Electronics, Vol. 43, No. 1, Feb. 1996, pp. 56-64

[8] R. Dhaouadi, K. Kubo, and M. Tobise, “Analysis and Compensation of Speed Drive Systems with Torsional Loads”, IEEE Transactions on Industrial Applications Society, Vol. 30, No. 3, May/Jun. 1994, pp. 760-765

[9] J. Tal, “Resonance and Backlash Compensation with Continuous Dual Loops”, Motion, Mar./Apr. 1993, pp. 14-18

[10] M. Odai and Y. Hori, “Speed control of 2-inertia system with gear backlash using gear torque compensator”, Advanced Motion Control, AMC '98-Coimbra., 5th International Workshop on , 29 June-1 July 1998, pp. 234-239

[11] S. Bolognani, K. Unterkofler, M. Zigliotto, M. Zordan, “Computer-aided commissioning of electrical drives for two-mass-systems with mechanical imperfections”, Proceedings of the IEEE International Symposium on Industrial Electronics, ISIE '99, Vol. 3, 12-16 July 1999, pp. 1339-1344

[12] J.C. Gerdes, V. Kumar, “An impact model of mechanical backlash for control system analysis”, Proceedings of the American Control Conference, 1995, Vol. 5, 21-23 June 1995, pp. 3311-3315

[13] P. Schmidt and R. Lorenz, “Design Principles and Implementation of Acceleration Feedback to Improve Performance of DC Drives“, IEEE Transactions on Industrial Applications, May/Jun. 1992, pp. 594-599

[14] J. Deur and N. Peric, “A Comparative Study of Servosystems with Acceleration Feedback”, Proceedings of IEEE Industrial Applications Society Annual Conference, Rome, Italy, 2000, pp. 1533-1540

[15] S. Valiviita and O. Vainio, “Delayless Differentiation Algorithm and Its Efficient Implementation for Motion Control Applications”, IEEE Transactions on Instrumentation and Measurement, Vol. 48, No. 5, Oct. 1999, pp. 967-971